THE SUPERNOVA ORIGINS OF RARE STARDUST ENRICHED WITH ^{13}C AND ^{15}N . J. Schulte[1,2,*], M. Bose[1,*], P. Young[1], and G. Vance[1], [1]School of Earth and Space Exploration, Arizona State University, Tempe, AZ 85287-6004. [2]Department of Physics, Arizona State University, Tempe, AZ 85287-1504. *Center for Isotope Analysis (Maitrayee.Bose@asu.edu)

Introduction: SiC presolar grains, or stardust have condensed in a variety of astrophysical environments, and have been categorized based on the isotope signatures of the grains. Stardust with large ^{13}C and ^{15}N excesses relative to solar ^{12}C/^{13}C and ^{14}N/^{15}N ratios have been given several names in the literature, including "putative nova grains" [e.g., 1], "nova candidate grains" [e.g., 2], and simply "nova grains" [e.g., 3-4]. Although a few grains may have nova origins [5], their classification necessitated some assumptions, e.g., mixing of nova ejecta with the surrounding medium. For these reasons along with the additional evidence for a core-collapse supernova (SN) origin (this work) we relabel these grains with large ^{13}C and ^{15}N excesses as SiC 'D' grains.

Here, we compare new three-dimensional SN model predictions to the compositions of SiC D grains, discuss the physical reasons for the production of low carbon and nitrogen ratios in the grains, and additional implications of the explosion that can explain the SiC D grain isotope systematics.

Methods: In this work, we use the isotope yields, from two three-dimensional supernova models. These models, previously labeled as jet3b and 50Am [6], will hereafter be referred to as 15A and 15S. 15A is an asymmetric 15 $M_\odot$ explosion, whereas 15S is a spherically symmetric explosion of the same mass. Both models are first run through the 1D stellar evolution code TYCHO [7] until core collapse, which is handled by 1D Lagrangian code [8]. After core bounce, the SN shockwave is revived by an energy injection following the method laid out by Fryer et al. [9]. After shock revival, the results are mapped into the 3D smoothed particle hydrodynamics (SPH) code SNSPH [10]. The models are then post-processed using the Burnf code [11] to obtain accurate isotope yields. Finally, output files are generated containing positional data of each SPH particle along with their mass, density, smoothing length and isotope mass fractions. Each simulation contains roughly one million SPH particles, having an average mass of 1.7 earth-masses. To reflect this large mass and avoid confusion, we will hereafter refer to each SPH particle as a "clump" of material. The location (usually with respect to the X-Z plane), temperature and density of the clumps were further explored to understand nucleosynthesis during explosion.

Preliminary work using these 3D SN models [6], 15S and 15A included an abundance cutoff of 10^{-6} (i.e., only isotopes with mass ratios > 10^{-6} had non-zero values). The clumps with mass fractions below 10^{-6} matched the nitrogen isotopic compositions of the X and D grains, but could not capture the carbon isotope ratios [6]. This bias was caused by use of a low-abundance cutoff, which is done to limit the size of output files and exclude particles with exceptionally small abundances. For the purpose of investigating ^{13}C and ^{15}N enriched clumps, this abundance cutoff was lowered to a minimum mass fraction of 10^{-10}. This same cutoff was then used for all isotopes discussed here.

The SiC stardust isotope data used here were obtained from the presolar grain database, which is maintained by the Washington University in St. Louis [12]. Additional data sources used were [1, 5, 13]. The stardust isotopic measurements from these sources and the model data were analyzed using MATLAB and the SPH visualization tool SPLASH [14].

Results and Discussion: Using the lower abundance cutoffs, the two 15 $M_\odot$ SN models were able to reproduce both the carbon and nitrogen isotope compositions of SiC D grains (Figure 1). Both the symmetric and asymmetric model predicted similar carbon and nitrogen compositions to most SN grains and several SiC D grains.

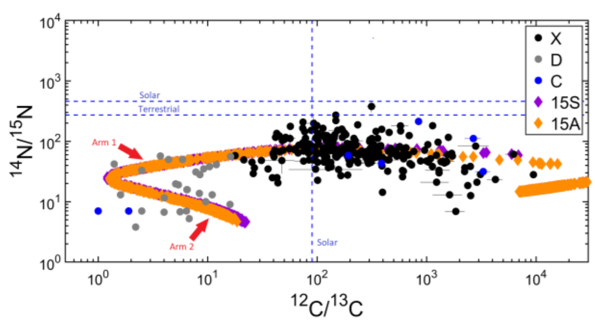

Figure 1: Carbon and nitrogen isotopic compositions of SiC X, D, and C grains in comparison to modeled isotope yields from two 15 $M_\odot$ models, 15A and 15S.

Using the spatial distribution of the clumps, we determined that large ^{13}C and ^{15}N enrichments are possible only deep within the interior of the explosion. Figure 2 plots the clumps 43 hours after the explosion in the 15S model, which clearly shows that the clumps with low C isotopic ratios form within the inner-most Si/S or Ni zones in a pre-SN star. The same region also contains the clumps with low ^{14}N/^{15}N ratios (< 65). Spatially, there is no difference between the 2 features (labelled arms 1 and 2) models in the 3rd quadrant of Figure 1.

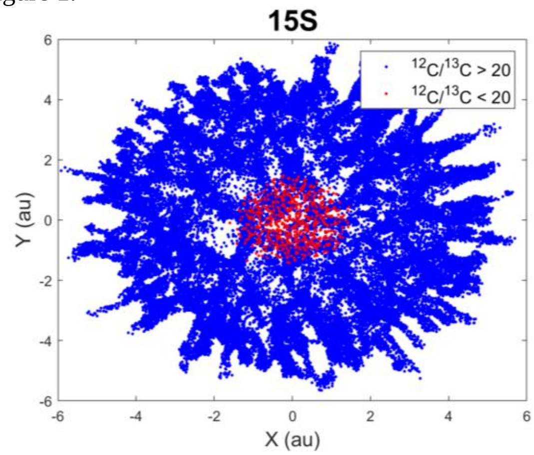

Figure 2: Spatial plot of the X-Y plane of the spherically symmetric explosion 15S 43 hours after core collapse. Clumps shown in red have similar C and N compositions to SiC D grains.

Since this material is forming in the interior of the explosion, clumps in this region of the explosion have temperatures above 10^8 K and densities higher than 23 g cm^{-3} for the first 33 seconds after core collapse. Because of these high temperatures, ^{13}C in these clumps is efficiently produced through rapid proton capture defined by the reaction $^{12}C(p,\gamma)^{13}N(\beta^+)^{13}C$. The enrichments in ^{15}N are further enabled at high temperatures and densities through the presence of ^{13}C nuclides, enabling the CNO cycle and leading to the reaction $^{14}N(\alpha,\gamma)^{18}F(p,\alpha)^{15}O(\beta^+)^{15}N$.

Next, we investigated several heavier isotopic abundances, including the stable isotopes of silicon, ^{28}Si, ^{29}Si, and ^{30}Si and the short-lived radionuclide (SLR) ^{26}Al. While SiC D grains usually have solar ^{29}Si abundances, they have enrichments in ^{30}Si with respect to ^{28}Si that can be as high as $\delta^{30}Si/^{28}Si$ = 1118 ‰ [15]. Modeled clumps with $^{12}C/^{13}C < 20$, however, predict much larger enrichments of both ^{29}Si and ^{30}Si, in the range of 3800 to 6200 ‰ for ^{29}Si and 18000 to 34000 ‰ for ^{30}Si. This is because the material, so close to the center of the SN, is first enriched with ^{28}Si from explosive oxygen burning until the shockwave carries with it a large amount of free neutrons, bombarding the ^{28}Si nuclides and producing heavier stable isotopes of Si. The ^{30}Si enrichments observed in SiC D grains might be the result of these ^{29}Si nuclides undergoing further neutron capture.

Compared to stardust grains of AGB star and J-type star origins, SiC D grains have relatively large $^{26}Al/^{27}Al$, generally between 0.01 and 0.4. The modeled clumps with $^{12}C/^{13}C < 20$, due to the ^{26}Al-rich environment of a core-collapse SN, also have large $^{26}Al/^{27}Al$, between 0.3 and 0.6 in the interior of the explosion (Figure 3). These high ^{26}Al abundances, produced in the same region of the explosion as the ^{13}C excesses, are possible for the same reason ^{13}C excesses are possible: high temperature and density in the interior of the explosion allow for rapid proton capture onto the isotope ^{25}Mg. Large ^{25}Mg abundances in the interior of the SN therefore allow the formation of ^{26}Al via the reaction $^{25}Mg(p,\gamma)^{26}Al$.

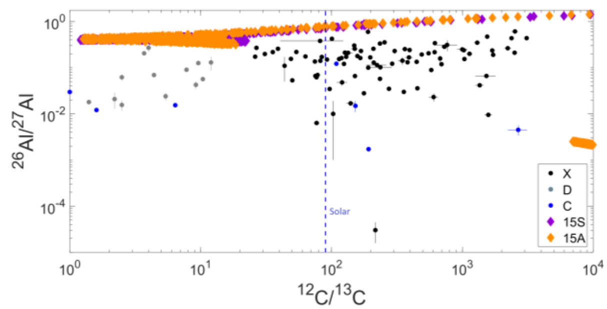

Figure 3: Carbon and aluminum compositions of SiC X, D, and C grains compared to modeled isotope yields from SN simulations 15S and 15A.

Finally, we investigated the isotopes of sulfur and titanium and determined that the interior of both modeled explosions contain ^{33}S, ^{34}S, and ^{44}Ti nuclides and both models can explain the sulfur compositions of SiC D grains. Additional high-precision sulfur and titanium isotope analyses of SiC grains are required to constrain the models further.

Conclusions: We demonstrate that presolar SiC D grains condense deep within the interior of a 15 $M_{\odot}$ core-collapse supernova, and require rapid and explosive proton burning. Both 15S and 15A simulations predict that SiC D grains should show evidence of fast neutron capture as a result of the neutron-rich environment in the inner-most regions of the supernova.

References: [1] N. Liu et al. (2016) *ApJ* 820, 140-153. [2] J. José and M. Hernanz (2007) *Meteorit. & Planet. Sci.* 42, 1135-1143. [3] S. Amari et al. (2001) *ApJ* 551, 1065-1072. [4] E. Zinner. (2014) *Meteorit. & Cosmochem. Proc.* Treat. On Geochem. 1, 181-213. [5] M. Bose and S. Starrfield. (2019) *ApJ* 873, 14-27. [6] J. Schulte et al. (2019) *LPSC L*, Abstract #1746. [7] P. A. Young and D. Arnett. (2005) *ApJ* 618, 908-918. [8] M. Herant et al. (1994) *ApJ* 435, 339-361. [9] C. L. Fryer et al. (2018) *ApJ* 856, 63-76. [10] C. L. Fryer et al. (2006) *ApJ* 643, 292-305. [11] P. A. Young and C. L. Fryer (2007) *ApJ* 664, 1033-1044. [12] K. M. Hynes and F. Gyngard. (2009) *LPSC XL*, Abstract #1198. [13] K. K. Marhas et al. (2008) *ApJ* 689, 622-645. [14] D. J. Price. (2007) *PASA* 24, 159-173. [15] X. Gao and L. R. Nittler (1997) *LPSC XXVIII*, Abstract #1769.